Catalysis Science & Technology

PAPER

View Article Online
View Journal | View Issue

Cite this: *Catal. Sci. Technol.*, 2014, 4, 786

High performance $(VO_x)_n$–$(TiO_x)_m$/SBA-15 catalysts for the oxidative dehydrogenation of propane†

Carlos Carrero,[ab] Markus Kauer,[a] Arne Dinse,[ac] Till Wolfram,[d] Neil Hamilton,[d] Annette Trunschke,[d] Robert Schlögl[bd] and Reinhard Schomäcker*[a]

Received 23rd August 2013,
Accepted 12th December 2013

DOI: 10.1039/c3cy00625e

www.rsc.org/catalysis

Grafted V_xO_y catalysts for oxidative dehydrogenation of propane (ODP) have been studied due to their potential high performance and as model catalysts in the past. We report on a positive synergetic effect capable of considerably enhancing the propene productivities above reported performances. The most productive catalysts were found at metal loadings (V + Ti) close to the monolayer coverage. The 4V/13Ti/SBA-15 catalyst presented a considerably high productivity (6–9 $kg_{propene}$ kg_{cat}^{-1} h^{-1}). Moreover, with this catalyst, propene productivity only slightly decreased as a function of propane conversion, indicating that propene combustion toward CO_x occurs more slowly in comparison to other catalysts exhibiting high propene productivities. A detailed kinetic analysis of the 4V/13Ti/SBA-15 catalyst revealed that high vanadia and titania dispersions are required for high propene productivity.

1 Introduction

The chemical industry is largely based on the conversion of alkenes as they are versatile raw materials that may be easily and economically obtained from petroleum.[1] Partial oxidation of low molecular weight alkanes (from C1 to C4), with the focus on oxidative dehydrogenation and oxo-functionalization as target reactions, has been studied extensively.[2,3] As the demand for propene is growing faster than the demand for either ethylene or gasoline, there is a widening gap between propene demand and that which may be supplied *via* conventional routes, *i.e.* catalytic (FCC) and steam cracking or direct dehydrogenation of propane.[4] Oxidative dehydrogenation of propane offers several advantages over traditional routes, such as: being thermodynamically less restrictive; lower reaction temperatures; no catalyst deactivation due to coke deposition; and less overall energy demand and therefore lower running costs.

For the reasons given above, ODP is an attractive solution to bridge the propene supply–demand gap.[5]

Since propene is more reactive than propane,[6] consecutive combustion reactions lead to poor propene yields. Thus, improving the selectivity toward propene is the main challenge to overcome for developing ODP as a commercially viable process. Vanadium-based catalysts are frequently applied as oxidation catalysts in industry.[7] Among other reactions, they are known to be active for the oxidative dehydrogenation of light alkanes.[5,8] ODP is facile on oxides of vanadium, molybdenum, and chromium with vanadia-based catalysts typically providing higher rates and propene selectivities.[9] Recently, carbon nanotubes as well as subnanometer platinum clusters have been presented as attractive alternatives to metal oxide catalysts for ODP.[10,11]

It has been proposed that ODP over vanadia-based catalysts occurs under participation of lattice oxygen as was evidenced by isotopic tracer studies.[12] Theoretical studies corroborate the fact that lattice oxygen is involved in the ODP catalytic cycle.[13] As a consequence, detailed studies have been performed considering the influence of vanadia loading,[8,14] the effect of the material support[5,8,15,16] and the influence of a vanadium oxide precursor[17] on the overall ODP reaction rate. Table 1 summarizes the findings of these studies.

While it was found that TiO_2-supported vanadium oxide has the highest turnover frequency (TOF), it also shows the lowest surface area.[18]

Table 1 Surface areas, composition, propene selectivity at isoconversion (~5%), and ODP reactivity comparison of different vanadium supported catalysts at 500 °C

	BET (m^2 g^{-1})	V nm^{-2}	TOF [10^{-3} s^{-1}]	Selectivity [%]	Ref.
V/Al_2O_3	109	1.5	26	67	20
V/SiO_2	300	1.4	11	67	21
V/TiO_2	51	1.8	126	30	16
V/ZrO_2	74	2.8	60	—	18
V/MgO	101	3.1	9	31	16

[a] *Department of Chemistry, Technical University of Berlin, Strasse des 17. Juni 124, 10623 Berlin, Germany. E-mail: schomaecker@tu-berlin.de*
[b] *Department of Heterogeneous Catalysis, MPI-CEC, Stiftstr. 34-36, D-45470, Mülheim, Germany*
[c] *BP North America, 150 W Warrenville Road, Naperville, 60563 IL, USA*
[d] *Department of Inorganic Chemistry, Fritz Haber Institute of the Max Planck Society, Faradayweg 4-6, 14195 Berlin, Germany*
† Electronic supplementary information (ESI) available. See DOI: 10.1039/c3cy00625e

In turn, this leads to a limited concentration of dispersed surface vanadium sites,[19] which are essential for optimal propene selectivity, and, therefore, low propene productivities. On the other hand, SiO_2 support material, owing to its high surface area (~300–1500 $m^2\ g^{-1}$), is the best candidate to prepare catalysts with a high abundance of VO_x surface sites. The disadvantage of utilizing SiO_2 is the hydrolytic sensitivity of V–O–Si bonds that leads to segregation of vanadia under the influence of the co-reaction product water.

Thus, utilization of a mixed oxide support that combines the beneficial properties of both SiO_2 and TiO_2 constitutes a promising approach towards the improvement of propene productivity in ODP. Previous studies have found that ternary $(VO_x)_n$–$(TiO_x)_m/SiO_2$ catalysts have demonstrated superior catalytic performance in various selective oxidation reactions.[22–25] In other studies focusing on productivity towards propene, a comparison of the performance of several vanadium oxide-based catalysts for ODP has already been reported.[5] The maximum reported propene productivity obtained from a vanadia based catalyst is 1.8 kg C_3H_6 kg_{cat}^{-1} h^{-1}.[26] Even higher propene productivities (9.3 kg C_3H_6 kg_{cat}^{-1} h^{-1}) have been obtained only by working under severe reaction conditions with total oxygen conversion.[27] While such experiments indicate the potential of a catalyst, they cannot be maintained under practical operation conditions as the catalyst lifetime will be greatly reduced for a number of reasons.

In our previous study, we attempted to optimize propene productivities by tuning the relative surface concentrations of titanium and vanadium oxide species supported on SBA-15.[28] The primary aim was to understand the synthesis and surface topology of the silica supported catalysts. From the library of mixed $(VO_x)_n$–$(TiO_x)_n$/SBA-15 catalysts, those catalysts containing metal loadings close to the monolayer coverage for the particular SiO_2 support (approx. 17 wt%) showed considerably high and industrially attractive propane productivities. In the present work, we study the kinetics of propane ODH over the 4V/13Ti/SBA-15 catalyst as it exhibits, besides high propene productivity, a slower propane combustion rate. The goal of present macro kinetic studies is to evaluate dependencies of ODP rates on reaction conditions (temperature, concentrations, pressure and flow rates). The resulting model will provide data for the design of a suitable reactor and the optimization of its operation.

2 Experimental

2.1 Catalyst synthesis and characterization

The catalysts were prepared by grafting alkoxide precursors as is described in detail in ref. 27. Although Santa Barbara mesoporous silica (SBA-15) has a lower surface area than MCM materials (~800–1000 $m^2\ g^{-1}$),[29] it was selected for this study because it exhibits a higher thermal stability than the thinner-walled MCM-41.[30] The 4V/13Ti/SBA-15 catalyst has been characterized by nitrogen adsorption; FTIR, Raman and UV-vis spectroscopy; thermal analysis; and *in situ* near edge X-ray absorption fine structure (NEXAFS) spectroscopy, and the results have been described previously.[28]

2.2 Kinetic measurements

All catalytic measurements were performed at ambient pressure using U-shaped fixed bed quartz reactors (i.d. 6 mm). The pristine powder catalysts were pressed and sieved to a particle size in the range of 200–300 μm. In order to avoid hot spots and to homogenize the temperature gradient inside the catalyst bed, the catalyst particles were diluted with inert silicon carbide (SiC) of the same particle size in the mass ratio 1 : 2 (catalyst/SiC). The reactor, containing the diluted catalyst between two layers of silicon carbide, was immersed into a fluidized bed of sand serving as a heat source 8 cm long under isothermal conditions. The reactant feed consisted of synthetic air (20.5% O_2 in N_2) and propane (99.9% C_3H_8). The flow rates of the reactant gases (C_3H_8, synthetic air) were controlled by two mass flow controllers (Bronkhost Hi-Tech, E1). The reactant mixture passed a static mixer prior to entering the reactor. The feed and the product components leaving the reactor were analyzed using an on-line gas chromatograph (GC, Shimadzu 2014) equipped with two packed columns (HayeSep Q and molecular sieve 13×) for the separation of O_2, N_2, CO, CO_2, and C^{1+} gases. Oxygen and nitrogen were detected by a thermal conductivity detector, whereas hydrocarbons and methanized carbon oxides were detected by a flame ionization detector. The steady state conditions were achieved after a maximum of 30 minutes. Bare support reactivity using *d*Ti/SBA-15 (*d* = 0–23 wt% Ti) catalysts was also measured. Experiments using pure SiC were carried out demonstrating the absence of homogeneous gas phase reaction below 550 °C. The conversion and selectivity were calculated based on the total number of carbon atoms and the products found. The carbon balance was close up to 100 ± 5%. For more experimental details, see ref. 35.

Depending on the purpose, the experiments were designed as follows:

2.2.1 $(VO_x)_n$–$(TiO_x)_n$/SBA-15 matrix: impact of the V : Ti ratio on propylene productivity[28]. The experiments were performed in the temperature range 440–520 °C. Propane conversion was maintained below 10% to ensure a gradientless reactor. Besides, total oxygen conversion was avoided. The catalyst mass and the total flow rates were varied in the range 1–300 mg and 20–100 cc min^{-1}, respectively. These experiments served as the first step to select the 4V/13Ti/SBA-15 catalyst as a candidate for further kinetic studies.

2.2.2 Catalyst 4V/13Ti/SBA15: apparent ODP activation energy. The experiments were carried out at temperatures in the range 380–520 °C. For temperatures below 460 °C, 30 mg of catalyst was used, while 5 mg of catalyst was required for the higher reaction temperatures. Using a fresh catalyst, two different experiments were identically performed in order to prove the reproducibility and accuracy of the measurements.

2.2.3 Catalyst 4V/13Ti/SBA15: determination of reaction orders. For this purpose, the reactant feed composition was

varied between eight different $C_3H_8:O_2$ ratios (3:1, 2:1, 1.5:1, 0.5:1, 1:1, 1:2, 1:3, and 1:4). Several experiments were carried out at 400 °C and atmospheric pressure, varying the catalyst mass from 15 to 60 mg. O_2 and N_2 were fed separately at specific flows to achieve the desired feed composition. After finishing one experiment at a specific $C_3H_8:O_2$ ratio, and before measuring the catalytic activity at a new feed composition, the catalyst was completely oxidized at 400 °C (60 mL min^{-1} of synthetic air).

2.2.4 Catalyst 4V/13Ti/SBA15: time on stream catalyst stability. In order to demonstrate the stability of our catalyst under ODP reaction conditions, *i.e.* where oxygen conversion is restricted to below 100%, we used 10 mg of the catalyst following the same procedure described above. Reaction temperature was 500 °C and the modified residence time was invariable at 6 kg_{cat} s m^{-3}.

3 Results and discussion

3.1 Catalyst synthesis and characterization

The applied grafting method provided a high metal dispersion up to monolayer coverage as shown elsewhere. The distribution of vanadia and titania species coexisting on the surface of SBA-15 is illustrated in Scheme 1.[28] The BET surface area of all catalysts varies in the range between 270 and 980 m^2 g^{-1}.

The surface of 4V/13Ti/SBA-15 is characterized by a monolayer that covers the silica almost entirely. UV-vis and NEXAFS spectroscopy reveal unique spectroscopic features that may be interpreted in terms of a joint V–Ti oxide monolayer. In this joint monolayer, the abundance of V–O–V and V–O–Ti bonds is maximized and oligomers with mixed nuclearity are formed, which is reflected by the peculiar electronic and catalytic properties of the material.[28]

3.2 Oxidative dehydrogenation of propane

3.2.1 Impact of the V:Ti ratio. As shown in Fig. 1 for catalysts containing 4% V (Fig. 1a), the reactivity increases with increasing loading of titanium oxide.

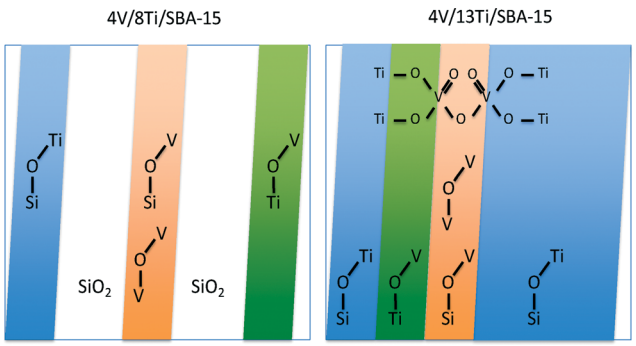

Scheme 1 Schematic illustration of the different surface topologies of V–Ti sub-monolayer catalysts, like 4V/8Ti/SBA-15, and V–Ti monolayer catalysts, like 4V/13Ti/SBA-15, including all topological features evidenced by spectroscopic techniques (white area: free silica surface, blue area: surface area covered by titanium oxide surface species, green area: vanadium oxide species supported on dispersed titania species, orange area: dispersed vanadia species on the silica surface).[28]

At low titanium loadings (below 13 wt%), the reaction rate is very low, whereas at higher titanium oxide loadings (above 13 wt%), it is remarkably enhanced (Fig. 1a). On a support that contains a monolayer of titanium oxide species (17 wt% Ti), the rate increases with increasing vanadium oxide loading (Fig. 1b), indicating that vanadium oxide is the catalyst component that is mainly responsible for the catalytic activity.

Vanadium oxide supported on monolayer or multilayer titania, such as in the catalysts 4V/17Ti/SBA-15 and 4V/23Ti/SBA-15, respectively, presents the highest rates of propane consumption, confirming that vanadium oxide supported on titanium oxide shows high activity.[27] Since a certain loading of titanium oxide is required to remarkably improve the ODP rates using the ternary catalysts studied here, and taking into account that vanadium-free TiO_2/SBA-15 catalysts exhibit very low activity in ODP, titanium oxide oligomers are promoters rather than a *bona fide* catalytic species. It is interesting to note that the rates are in the same order of magnitude for 4% V/SBA-15 and 17% Ti/SBA-15. This demonstrates a strong synergetic effect of V and Ti in the joint monolayer or bi-layered form.

Propene selectivity as a function of both vanadia and titania loading is depicted in Fig. 2 at a propane isoconversion of ~6% at 500 °C. There are no large differences observed in the

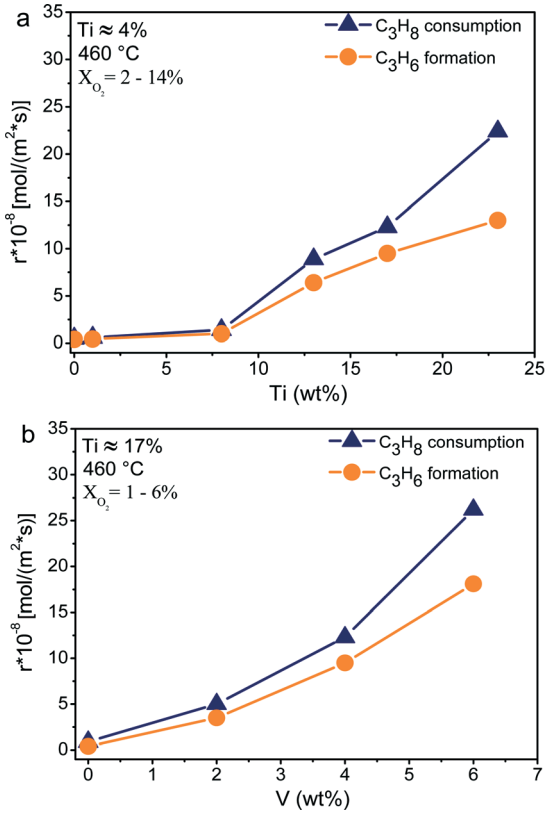

Fig. 1 Propane consumption and propene formation rates as a function of titania loading (a) and vanadia loading (b) at 460 °C. Catalyst mass: 5–50 mg. Total flow: 100 cc min^{-1}.

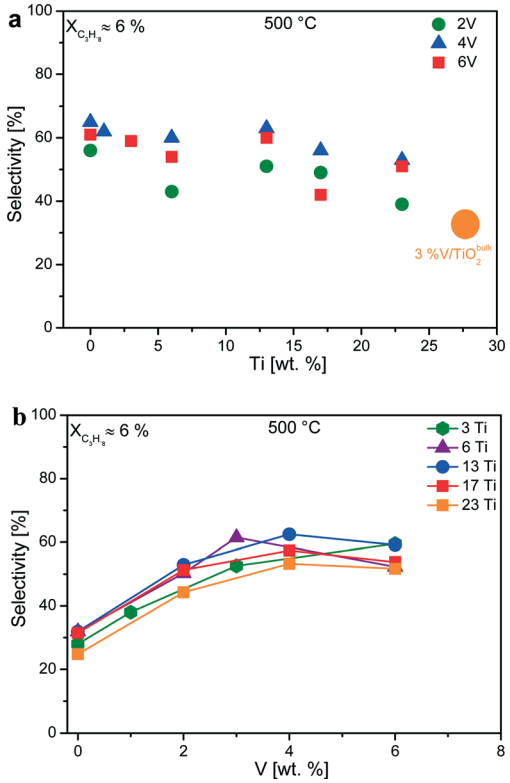

Fig. 2 Selectivity as a function of titania (a) and vanadia (b) loading at 500 °C. Catalyst mass: 2–150 mg, total flow rates: 120–20 ml min^{-1}, and $C_3H_8 : O_2 = 2$.

propene selectivity up to the point at which monolayer coverage of titania is reached at ~17 wt% Ti.

The 3% V/TiO_2 (anatase) catalyst is used as reference.[17] Apparently, using two-dimensional TiO_x species instead of bulk TiO_2 (Fig. 2a) is beneficial with respect to selectivity. This is also in agreement with the trend that becomes apparent in Fig. 2a and that shows a slightly lower selectivity for vanadia supported on 23Ti/SBA-15 that already contains a multilayer of TiO_x.

Irrespective of whether the silica surface is covered by a sub-monolayer of titania (range, between 3 and 13 wt% Ti), or whether monolayer or multilayer coverage of SiO_2 with TiO_x is existent (17 and 23 wt% Ti), the selectivity to propylene increases with increasing vanadia loadings up to 3 wt% V and then remains constant at higher V loadings (Fig. 2b). This observation is not easily explained assuming decoration of non-selective TiO_x sites by vanadia species, but rather suggests that a certain size of the vanadia oligomers is required to catalyze the ODH of propane selectively to propylene irrespective of the nature of the support. However, conclusions are difficult within the investigated catalyst matrix, because the structure and location of the vanadia species depend on the coverage of silica with titania.[28] For example, in the catalysts that contain 3Ti/SBA-15 as support, the titanium oxide species should be covered to a large extent by vanadium oxide, because VO_x is preferentially anchored on top of TiO_x on 3Ti/SBA-15.[28] In contrast, VO_x fills the free silica patches in the case of higher titania loadings, like 13 wt%, leading to the formation of a joint monolayer, but not a bi-layered catalyst in the case of 4V13Ti/SBA-15.[28] In any case, the results clearly indicate that monolayer titania species behave differently compared to bulk TiO_2 in ODH of propane. Since the selectivity to propylene over pure Ti catalysts is approximately 30% (Fig. 2b), it can be assumed that the Ti component itself is also participating in the propane dehydrogenation step over VTi/SBA-15 catalysts. For this reason, the rate expressions in this study (Fig. 1) as well as in our previous publication[28] are reported considering the BET surface area (surface related rates) rather than the vanadium oxide surface density (TOF).

Fig. 3 shows the propene selectivity as a function of reaction temperature for SBA-15, 6Ti/SBA-15, and 13Ti/SBA-15 as support. As expected, the propene selectivity increases with reaction temperature for all catalysts. Interestingly, the extent of the temperature dependence decreases with increasing Ti loadings, indicating a gradual structural influence of titania on the catalytic properties of the vanadium oxide species, reducing the difference between the activation energies of ODP and total oxidation of propene.

Catalysts containing TiO_2 anatase nanoparticles (nV/23TiO_2) show considerably low propene selectivities at zero propane-conversion intersections (56–61%), further indicating that TiO_2 nanoparticles not only accelerate parallel propene combustion reactions but also catalyze the direct combustion of propane towards CO and CO_2.

Fig. 4 illustrates the synergistic effect of the V–Ti interaction with respect to the productivity of the catalysts. At low titania loadings, the enhancement of propene productivity is almost negligible, indicating that a considerable fraction of the supported vanadium atoms is located on the residual titanium-free silica surface in the form of highly-dispersed oxide species characterized by low nuclearity.[27] At titanium loadings higher than 13 wt%, propene productivity is greatly enhanced. The productivity decreases linearly as the propane conversion increases since the consecutive total oxidation of propylene contributes increasingly at higher propane conversions. Assuming that carbon oxides are mainly formed by post-combustion of propylene, the slope of the productivity/conversion plots can be interpreted in terms of a ratio of the rate of propene formation *versus* the rates of subsequent propylene oxidation towards CO and CO_2.

The gradients for the most productive catalysts, 4V/13Ti/SBA-15, 4V/17Ti/SBA-15, and 4V/23Ti/SBA-15, are −0.5, −1.2, and −2.5, respectively, indicating that unselective post-combustion is most efficiently suppressed in the catalyst 4V/13Ti/SBA-15 that forms a joint VO_x–TiO_x monolayer. These ratios are presented separately in Fig. 4b. The fastest propene oxidation takes place on the 4V/23Ti/SBA-15 catalyst (Fig. 4). This high rate of total oxidation is attributed to the presence of TiO_2 nanoparticles.[27] Due to the superior propene productivity and high propene/CO_2 ratio of the catalyst 4V/13TBA-15 (Fig. 4), we determined the kinetic parameters in the oxidative dehydrogenation of propane using this catalyst. As shown in Fig. 5, the 4V/13Ti/SBA-15 catalyst also shows acceptable stability at

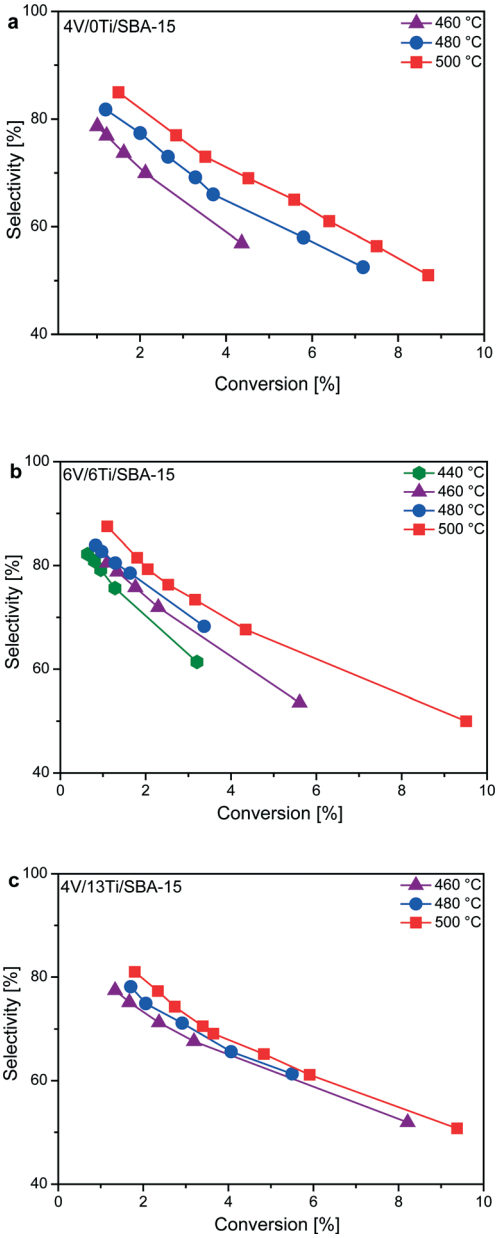

Fig. 3 Selectivity–conversion trajectories at different temperatures for (a) 4V/0Ti/SBA-15, (b) 6V/6Ti/SBA-15 and (c) 4V/13Ti/SBA-15. Experimental conditions for all the presented data are in the following ranges: catalyst mass: 2–150 mg, total flow rates: 120–20 ml min^{-1}, and $C_3H_8:O_2$ = 2. Selectivity for undesired products is found in the ESI,† Fig. S1–S2.

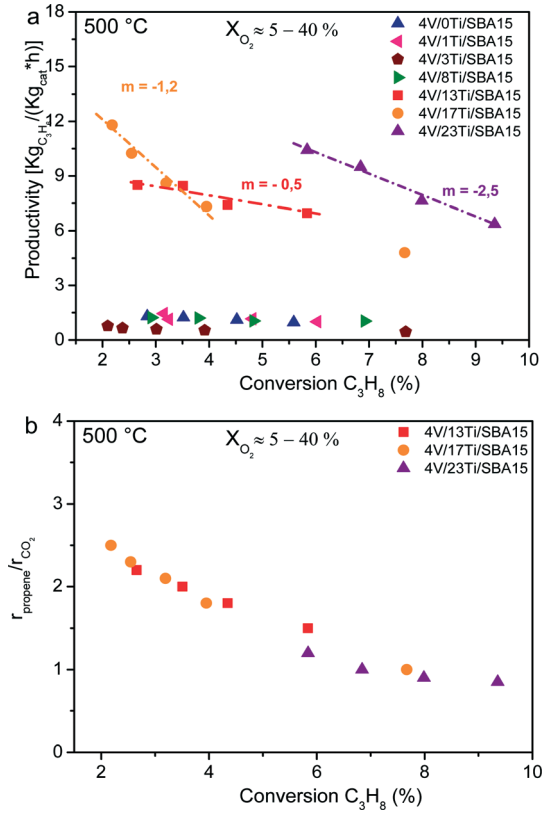

Fig. 4 Productivity (a) and ratio of propene formation and CO_2 formation rates (b) as a function of propane conversion at 500 °C over selected 4V/dTi/SBA-15 (d = 0–23 wt%) catalysts. Catalyst mass: 2–50 mg. Total flow: 20–140 cc min^{-1}. $C_3H_8:O_2$ ratio = 2.

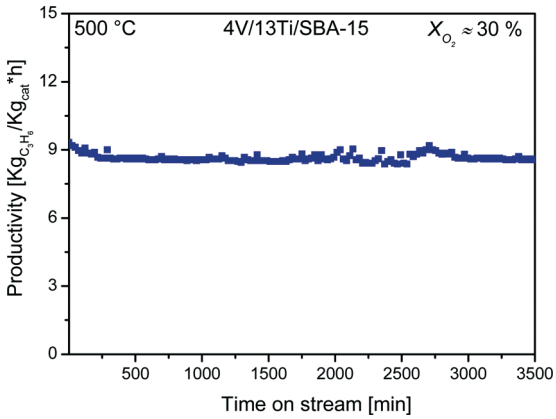

Fig. 5 Stability of 4V/13Ti/SBA-15 in terms of propene productivity as a function of time of stream at 500 °C. Catalyst mass: 10 mg. Total flow: 100 cc min^{-1}, $C_3H_8:O_2$ ratio = 2.

500 °C. This stability is reasonable since oxygen conversion is kept below 80% and therefore coke formation can be neglected.

3.2.2 Kinetic study of 4V/13Ti/SBA-15

This catalyst has been extensively characterized and it was found that both vanadia and titania are present in sub-monolayer concentrations without three-dimensional surface species of either V_2O_5 or TiO_2 anatase. Besides, as mentioned, the surface of 4V/13Ti/SBA-15 is characterized by a near monolayer coverage of supported metal oxide species. Previous findings indicate that when the combined total vanadium and titanium metal loading approaches monolayer concentration, vanadia species preferentially replenish the residual free silica surface functioning as polymeric bridging ligands between two polymeric surface titania domains.[27] Reference measurements employing a physical mixture of the 4V/SBA-15 and 13Ti/SBA-15 catalysts have shown that no

enhancement in catalytic activity (relative to the individual catalysts) was observed.

This clearly indicates the existence of a synergetic effect that requires chemical interactions between surface vanadium and titanium oxide species to yield improved catalytic activity.

In order to demonstrate this synergetic effect, the kinetic parameters of the reaction were determined for 4V/13Ti/SBA-14 and compared to 4V/SBA-15 and 1.7V/TiO_2. The applied experimental set-up and the evaluation methods are described in detail in ref. 35 and in the ESI.†

Measurements of initial reaction rates as a function of propane and oxygen partial pressures were performed in order to determine the reaction orders in propane and oxygen. The gradient of the resulting plots indicates that the reaction rates are first order in propane and zero order in oxygen (ESI,† Fig. S1). Thus, the reaction rate is directly proportional to the concentration of propane and it does not depend on the oxygen concentration, indicating that only propane is involved in the rate-determining step.[31] The observed zero reaction order with respect to oxygen indicates that the reaction rate is independent of oxygen concentration, which is consistent with the finding that reoxidation of the catalyst occurs much faster than propane oxidation (10^5 times).[32] It has been shown previously that when catalyst reoxidation is not the rate determining step of the overall reaction, the reaction order obtained for oxygen in formal kinetic approaches is low.[33] Due to propene being a stronger reducing agent than propane, the consecutive oxidation of propene cannot be studied separately to determine its reaction order.[34] As shown in Fig. 6, variation of the initial propane to oxygen ratios does not affect the propene selectivity at all. Therefore, it is reasonable to argue that the reaction orders of the consecutive propene combustion are also unity and zero for propene and oxygen, respectively. Similar reaction orders have been reported on different supported vanadia catalysts.[8,30,34] To the best of the authors' knowledge, no data concerning the reaction order for ODP on ternary $(VO_x)_n$–$(TiO_x)_m$/SBA-15 catalysts have previously been reported.

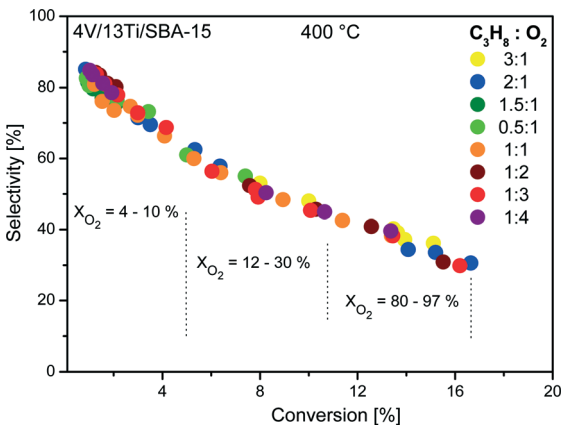

Fig. 6 Propene selectivity as a function of propane conversion at 400 °C and different initial propane/oxygen ratios. Catalyst mass: 7–60 mg. Total flow: 20–100 cc min^{-1}.

The course of the trajectory in Fig. 6 and its intercept at the selectivity axis at nearly 91% indicate that the consecutive total oxidation of propene to CO_x is the predominant side-reaction within the reaction network, determining the selectivity for propene (Scheme 2) in agreement with V/SBA-15 and V/TiO_2 catalysts studied in the oxidative dehydrogenation of propane before.[34,35] The ODP reaction network contains essentially the following parallel and consecutive reactions:[8]

$$C_3H_{8(g)} + V_2{}^{5+}O_{(s)} \rightarrow C_3H_{6(g)} + H_2O_{(g)} + V_2{}^{4+}{}_{(s)} \quad (A)$$

$$C_3H_{8(g)} + (4 + 3x)V_2{}^{5+}O_{(s)} \rightarrow 3CO_{x(g)} + 4H_2O_{(g)} + (4 + 3x)V_2{}^{4+}{}_{(s)} \quad (B)$$

$$C_3H_{6(g)} + (3 + 3x)V_2{}^{5+}O_{(s)} \rightarrow 3CO_{x(g)} + 3H_2O_{(g)} + (3 + 3x)V_2{}^{4+}{}_{(s)} \quad (C)$$

$$O_{2(g)} + 2V_2{}^{4+}{}_{(s)} \rightarrow 2V_2{}^{5+}O_{(s)} \quad (D)$$

Considering that no direct propane combustion takes place (very high propene selectivity at near zero propane conversion as shown in Fig. 6), the CO/CO_2 ratio does not depend on propane conversion as both products are formed simultaneously from the propene total oxidation.

The selectivity at zero conversion of more than 92% indicated a contribution of the propane total oxidation of less than 8%, which decreases with increasing propene formation due to the higher reactivity of propene. Therefore, the propane total oxidation reactions can be eliminated in a first approximation and the propene combustion can be lumped in one reaction resulting in the following rate expressions for ODP and consecutive propene combustion r_1 and r_2, respectively:

$$r_1 = k_{\infty,1}\exp(-E_{A1}/RT)C_{(C_3H_8)}^{(m_1)}C_{(O_2)}^{(m_2)} \quad (E)$$

$$r_2 = k_{\infty,2}\exp(-E_{A2}/RT)C_{(C_3H_6)}^{(m_3)}C_{(O_2)}^{(m_4)} \quad (F)$$

where k_∞, E_A and m are the pre-exponential factor, apparent activation energy and reaction orders.

The material balances for the stable reactants and products in a plug-flow tubular reactor are given by eqn (G)–(J) and were used for the one-dimensional modeling of the experimental data. From eqn (E) and (F), the oxygen concentration was omitted since the two reaction orders m_2 and m_4 are zero.

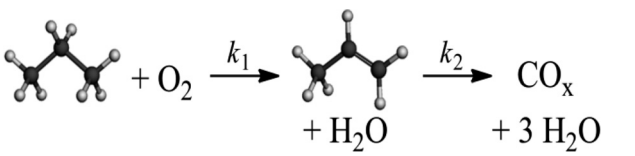

Scheme 2 The ODP reaction network.

$$dc_{C_3H_8}/d\tau = -r_1 \quad (G)$$

$$dc_{C_3H_6}/d\tau = r_1 - r_2 \quad (H)$$

$$dc_{CO_2}/d\tau = 3r_2 \quad (I)$$

$$dc_{O_2}/d\tau = 0.5r_1 - 3.5r_2 \quad (J)$$

The material balances were fitted to experimental data at six different residence times, six temperatures and eight different initial feed compositions with respect to propane and oxygen (Fig. 7). Fitting variables including the apparent activation energies for ODP and propene combustion, and the corresponding pre-exponential factors, $k_{1,\mathrm{eff}}$ and $k_{2,\mathrm{eff}}$, are summarized in Table 2. For the 4V/13Ti/SBA-15 catalyst, the ODP apparent activation energy obtained is 101 ± 2 kJ mol^{-1}. This value is between those determined for 4V/SBA-15 and 3V/TiO_2 catalysts (103 ± 6 and 78 ± 3 kJ mol^{-1}, respectively). This confirms the spectroscopic observation[28] that vanadia preferentially replenishes the residual free silica surface on the 4V/13Ti/SBA-15 catalyst surface (Scheme 1), forming a joint monolayer, but not a bi-layered catalyst. Otherwise, a lower activation energy closer to 78 ± 3 kJ mol^{-1} would have been expected. The increased abundance of V–O–Ti bonds in this specific surface confirmation results in higher productivities towards propene.[27]

The high reactivity accompanied by a low selectivity towards the desired product propene observed on V/TiO_2 catalysts has been attributed to the formation of both bulk and surface oxygen vacancies.[35] Recently, it was shown that oxygen vacancies can be formed in two-dimensional structures of TiO_2 supported on SiO_2 as well.[37] This may explain why 4V/13Ti/SBA-15 is considerably more active compared to V/SBA-15. On V/TiO_2, a low combustion activation energy E_{a2} (Table 2) reflects the facile combustion of propene towards carbon oxides, thereby decreasing the selectivity.

The advantage of a titanium oxide monolayer over bulk titania as the support material is ascribed to the balanced redox properties of VO_x in comparison to the high reducibility at bulk titania. This reduces the deep oxidation of the organic substrate due to the higher formation energy of oxygen vacancies in the two-dimensional oxides compared to bulk titania. The synergic relationship between the supported vanadium and titanium oxide species found in 4V/13Ti/SBA-15 increases the activation barrier to total oxidation of propene as well as the pre-exponential factors of all oxidation reactions in comparison to V/SBA-15 (Table 2). This observation provides a tuning parameter for the general concept of controlling the role of electrophilic lattice oxygen for optimizing the selectivity. The ternary catalyst 4V/13Ti/SBA-15 is not a V/TiO_2 catalyst spread on the high surface material SBA-15, with more active sites per BET surface area. It is a new catalyst with improved catalytic performance, caused by a higher number of active sites that increase the pre-exponential factors and a higher activation barrier for the total oxidation of the desired product propene, because of its tailored reducibility.

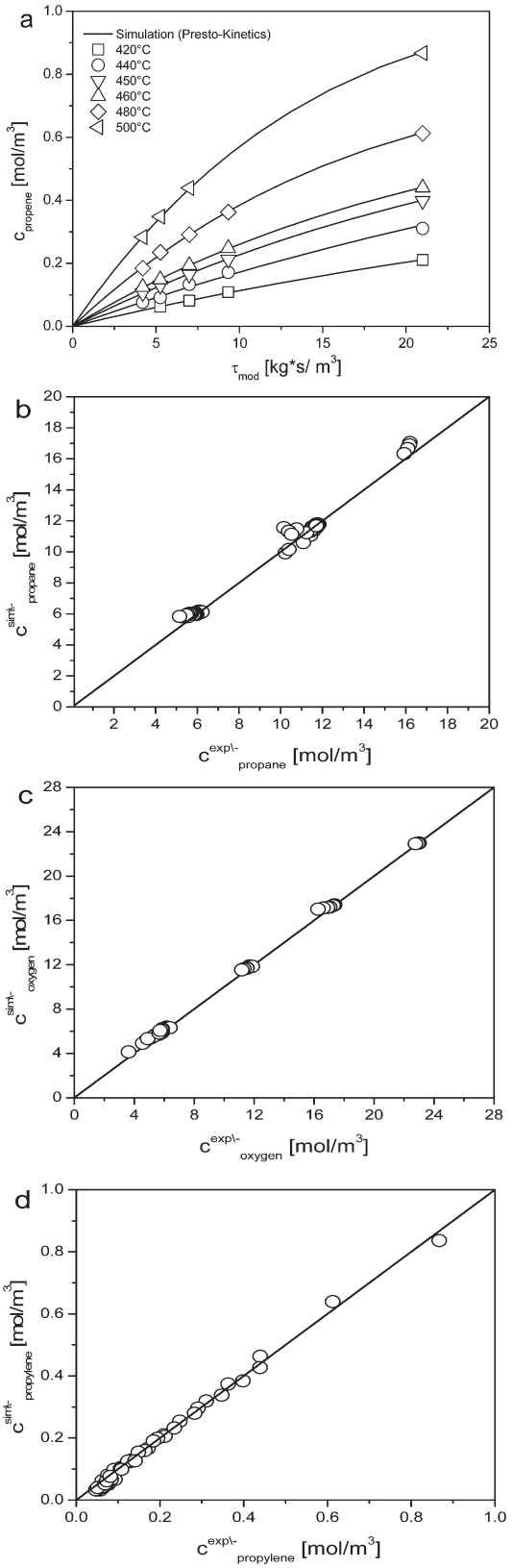

Fig. 7 (a) Propene concentrations as a function of modified residence times plus simulated trajectories at different reaction temperatures. Parity plots for simulated and experimental concentrations: (b) propane, (c) oxygen and (d) propene.

Table 2 Simulated kinetic data in the oxidative dehydrogenation of propane over different vanadia-based catalysts

Catalyst	V/TiO_2[a]	V/SBA-15[b]	V/Ti/SBA-15[c]
V (wt%)	1.7	2.7	4
Ti (wt%)	—	—	13.2
$k_{\infty,1}$ (m^3 mol^{-1} s^{-1})	—	101.2 ± 50.4	880 ± 440
$k_{\infty,2}$ (m^3 mol^{-1} s^{-1})	—	0.033 ± 0.013	22 ± 4.4
E_{a1} (kJ mol^{-1})	78 ± 3	103 ± 6	101 ± 2
E_{a2} (kJ mol^{-1})	39 ± 5	34 ± 18	57 ± 7
Rx order C_3H_8	1	1	1
Rx order O_2	0	0	0

[a] Ref. 36. [b] Ref. 35. [c] ESI, Fig. S4.

The structural reason may be the stabilization of two-dimensional oligomeric vanadium oxide species within the joint vanadia–titania monolayer that avoids the segregation of non-selective three-dimensional vanadium oxide nanoparticles. Non-stabilized V_xO_y is subject to such dynamics under conditions of the oxidative dehydrogenation of propane, through water as an unavoidable reaction product. Consequently, the measured synergic effect consists of two components, namely a structure-stabilization and an electronic modification of V_xO_y, with respect to the two borderline cases V/TiO_2 and V/SiO_2.

4 Conclusions and outlook

In conclusion, we have shown that ternary $(VO_x)_n/(TiO_x)_m$/SBA-15 catalysts at metal loadings close to the monolayer capacity of the SBA-15 support show productivities of propene that are around an order of magnitude greater than those reported so far, marking them as attractive candidates for industrial implementation. High vanadia dispersion is required to achieve high propene selectivity whereas formation of a joint V–Ti oxide monolayer is crucial to obtain improved reaction rates without sacrificing propene selectivity. In addition, operation of the catalyst under conditions that avoid total oxygen conversion is strictly necessary in order to guarantee long-term catalyst stability. Regarding the kinetic scheme of the reaction, some conclusions can be drawn that can aid the design of optimal reaction engineering for the ODP process applying this catalyst system. Since the by-products CO and CO_2 are only produced from the consecutive oxidation of propene, no reactor with back mixing behaviour like a fluidized bed should be chosen, although this type of reactor would certainly facilitate excellent isothermal conditions.

The substantially higher activation energy of ODP in comparison to the total oxidation of propene results in an increased propene selectivity with increasing temperature. This indicates that the reaction should be performed at a temperature as high as possible, up to a temperature where unselective gas phase reactions are excluded by choosing a compacted fixed bed reactor. Even at such temperatures, isothermal conditions could be realized in microstructured reactors with plug flow behavior as previously demonstrated for ODP,[19] enabling the highest possible performance of this catalyst. Our study has demonstrated new options for the design of improved monolayer grafted catalyst systems. In any case, it is essential that a full monolayer of the active component is achieved. As the highly active V_xO_y is on many supports subject to condensation reactions as a consequence of the high stability of iso-polyvanadates, it is essential that such oligomerisation is inhibited. There are a number of other cations forming sub-monolayer systems that can stabilize V_xO_y against oligomerisation which should allow a further decoupling of the oxidation of propane and propene. Tuning of the catalytic monolayer towards a weaker binding of propene should further increase the apparent activation barrier for the propene total oxidation. This should reduce the difference in reactivity of propane and propene to the minimum that is controlled by the difference in the weakest C–H bond strength. Research in such directions together with advanced deposition methods allowing for facile scale-up of catalyst synthesis are targets of synthetic research motivated by the high performance described in this communication.

Acknowledgements

The authors thank Torsten Otremba (TU-Berlin) and Klaus Friedel (Fritz Haber Institute, Berlin) for their help with both automatization and optimization of the reaction set-up. Special thanks to Dr. Olga Ovsitser (LIKAT – Rostock) for designing the experimental methodology and Prof. Israel Wachs (Lehigh University) for helpful discussions.

This work was supported by the German Research Foundation (Deutsche Forschungs-gemeinschaft, DFG) through the cooperative research center "Structure, dynamics, and reactivity of transition metal oxide aggregates" (Sonderforschungsbereich 546, http://www.chemie.hu-berlin.de/sfb546). Also, the authors thank Fundayacucho (Venezuela) – DAAD (Germany) PhD's scholarship program for basic funding.

References

1 G. Centi, F. Cavani and F. Trifiró, in *Selective Oxidation by Heterogeneous Catalysis*, ed. M. V. Twigg and M. S. Spencer, WILEY-VCH, New York, 2001, pp. 1–5.
2 R. Schlögl, in *Modern Heterogeneous Oxidation Catalysis*, ed. N. Mizuno, WILEY-VCH, Weinheim, 2009, p. 1.
3 (*a*) S. Arndt, G. Laugel, S. Levchenko, R. Horn, M. Baerns, M. Scheffler, R. Schlögl and R. Schomäcker, *Catal. Rev. Sci. Eng.*, 2011, **53**, 424; (*b*) C. Hammond, S. Conrad and I. Hermans, *ChemSusChem*, 2012, **5**, 1668.
4 A. Gallardo-Llamas, C. Mirodatos and J. Pérez-Ramírez, *Ind. Eng. Chem. Res.*, 2005, **44**, 455.
5 F. Cavani, N. Ballarini and A. Cericola, *Catal. Today*, 2007, **127**, 113, and references therein.
6 B. K. Hodnett, in *Supported Catalysts and Their Applications*, ed. D. C. Sherrington and A. P. Kybett, Royal Society of Chemistry, London, 2000, pp. 1–8.
7 B. Weckhuysen and D. E. Keller, *Catal. Today*, 2003, **78**, 25.
8 B. Frank, A. Dinse, O. Ovsitser, E. Kondratenko and R. Schomäcker, *Appl. Catal., A*, 2007, **323**, 66.

9 S. Yang, E. Iglesia and A. T. Bell, *J. Phys. Chem. B*, 2005, **109**, 8987, and references therein.
10 B. Frank, J. Zhang, R. Blume, R. Schlögl and D. S. Su, *Angew. Chem., Int. Ed.*, 2009, **48**, 1.
11 S. Vajda, M. Pellin, J. Greeley, C. Marschall, L. Curtiss, G. Ballentine, J. F. Mehmood and P. Zapol, *Nat. Mater.*, 2009, **8**, 213.
12 K. Chen, A. Khodakov, J. Yang, A. T. Bell and E. Iglesia, *J. Catal.*, 1999, **186**, 325.
13 (*a*) X. Rozanska, R. Fortrie and J. Sauer, *J. Phys. Chem. C*, 2007, **111**, 6041–6050; (*b*) X. Rozanska and J. Sauer, *Int. J. Quantum Chem.*, 2008, **108**, 2223.
14 H. Tian, E. Ross and I. Wachs, *J. Phys. Chem. B*, 2006, **110**, 9593.
15 D. Shee, T. V. Rao and G. Deo, *Catal. Today*, 2006, **118**, 288.
16 G. Marta, F. Arena, S. Coluccia, F. Frusteri and A. Parmaliana, *Catal. Today*, 2000, **63**, 197.
17 C. A. Carrero, C. J. Keturakis, A. Orrego, R. Schomäcker and I. E. Wachs, *Dalton Trans.*, 2013, **42**, 12644.
18 A. Lemonidou, L. Nalbandian and I. Vasalos, *Catal. Today*, 2000, **61**, 333.
19 R. Grabowski, *Appl. Catal., A*, 2004, **270**, 37.
20 O. Schwarz, D. Habel, O. Ovsitser, E. Kondratenko, C. Hess, R. Schomäcker and H. Schubert, *J. Mol. Catal. A: Chem.*, 2008, **293**, 45.
21 O. Ovsitser, M. Cherian and E. Kondratenko, *J. Phys. Chem. C*, 2007, **111**, 8594.
22 O. Ovsitser, M. Cherian, A. Brückner and E. Kondratenko, *J. Catal.*, 2009, **265**, 8, and references therein.
23 W. Vining, A. Goodrow, J. Strunk and A. T. Bell, *J. Catal.*, 2010, **270**, 163, and references therein.
24 X. Gao, S. Bare, J. L. Fierro and I. Wachs, *J. Phys. Chem. B*, 1999, **103**, 618, and references therein.
25 A. Comite, A. Sorrentino, G. Capannelli, M. Di Serio, R. Tesser and E. Santecesaria, *J. Mol. Catal. A: Chem.*, 2003, **198**, 151, and references therein.
26 E. Heracleous, A. Lemonidou and J. Lercher, *Appl. Catal., A*, 2004, **264**, 73.
27 O. Buyevskaya, A. Brückner, E. Kondratenko, D. Wolf and M. Baerns, *Catal. Today*, 2001, **67**, 369.
28 N. Hamilton, T. Wolfram, G. Müller, M. Hävecker, J. Kröhnert, C. Carrero, R. Schomäcker, A. Trunschke and R. Schlögl, *Catal. Sci. Technol.*, 2012, **2**, 1346.
29 P. Gruene, T. Wolfram, K. Pelzer, R. Schlögl and A. Trunschke, *Catal. Today*, 2010, **157**, 137.
30 J. Jarupatrakorn and T. Tilley, *J. Am. Chem. Soc.*, 2002, **124**, 8380.
31 A. Khodakov, J. Su, E. Iglesia and A. T. Bell, *J. Catal.*, 1998, **177**, 343.
32 K. Chen, A. Khodakov, J. Yang, A. T. Bell and E. Iglesia, *J. Catal.*, 1999, **186**, 325.
33 M. Argyle, K. Chen, E. Iglesia and A. T. Bell, *J. Phys. Chem. B*, 2005, **109**, 2414.
34 B. Frank, R. Fortrie, C. Hess, R. Schlögl and R. Schomäcker, *Appl. Catal., A*, 2009, **353**, 288.
35 A. Dinse, S. Khennache, B. Frank, C. Hess, R. Herbert, S. Wrabetz, R. Schlögl and R. Schomäcker, *J. Mol. Catal. A: Chem.*, 2009, **307**, 43.
36 R. Grabowski, J. Sloczynski and N. Grzesik, *Appl. Catal., A*, 2003, **242**, 297.
37 J. Strunk, W. Vining and A. T. Bell, *J. Phys. Chem. C*, 2010, **114**, 16937.

